Molecular Crystals and Liquid Crystals

Publication details, including instructions for authors and subscription information:
http://www.tandfonline.com/loi/gmcl20

LIQUID CRYSTALLINE PROPERTIES OF DISSYMMETRIC MOLECULES, PART XI: THE EFFECT OF ESTER AND LATERAL NITRO GROUPS ON THE MOLECULAR ARRANGEMENT IN SMECTIC PHASES IN THREE AROMATIC-RING SYSTEMS CONNECTED BY TWO ESTER GROUPS

Takcyasu Tasaka [a] , Hiroaki Okamoto [a] , Yuki Morita [a] , Kazuo Kasatani [a] & Shunsuke Takenaka [a]

[a] Department of Advanced Materials Science and Engineering, Faculty of Engineering, Yamaguchi University, Tokiwadai 2557, Ube, Yamaguchi 755-8611, Japan

Version of record first published: 15 Jul 2010

Mol. Cryst. Liq. Cryst., Vol. 404, pp. 15–31, 2003

ISSN: 1542-1406 print/1563-5287 online
DOI: 10.1080/15421400390249790

Taylor & Francis
Taylor & Francis Group

LIQUID CRYSTALLINE PROPERTIES OF DISSYMMETRIC MOLECULES, PART XI†: THE EFFECT OF ESTER AND LATERAL NITRO GROUPS ON THE MOLECULAR ARRANGEMENT IN SMECTIC PHASES IN THREE AROMATIC-RING SYSTEMS CONNECTED BY TWO ESTER GROUPS

Takcyasu Tasaka, Hiroaki Okamoto, Yuki Morita, Kazuo Kasatani, and Shunsuke Takenaka*
Department of Advanced Materials Science and Engineering, Faculty of Engineering, Yamaguchi University, Tokiwadai 2557, Ube, Yamaguchi 755-8611, Japan

The phase transition behavior and layer structure of 4-octyloxyphenyl 4-(4-alkoxy-3-X-benzoyloxy)benzoates and 4-(4-octyloxybenzoyloxy)phenyl 4-alkoxy-3-X-benzoates (X = H or NO_2) were examined by thermal, microscopic, and small-angle X-ray diffraction measurements. The homologs of the former (X = H) exhibit nematic, smectic A, and Smectic C (Sm A and C, respectively) phases, and the layer spacing shows a notable change near the Sm C–Sm A transition point, while in contrast the layer spacing for the homologs (X = NO_2) is almost independent of the phase transition and temperature. For the homologs of the latter (X = H and NO_2), on the other hand, the layer spacing is fairly narrow compared with the calculated molecular length, and it remains constant through the Sm A and Sm C phases. These results are discussed in terms of the layer structure of the Sm A and Sm C phases, and the molecular properties are obtained by a semi empirical molecular orbital calculation.

Keywords: liquid crystals; smectic properties; substituent effect; X-ray diffraction; smectic A-C phase transition

INTRODUCTION

It has been known that polarity, rigidity, and linearity are important factors in displaying liquid crystal (LC) properties. An ester group is one of the

Received 15 October 2002; accepted 22 July 2003.

†Part X of this series is T. Tasaka, H. Okamoto, Y. Morita, K. Kasatani, & S. Takenaka, Liquid Crystals, in press.

*Corresponding author. E-mail: oka-moto@po.cc.yamaguchi-u.ac.jp

useful functional groups in extending the LC core, since the dipole moment of the ester group, 1.90 D, and the single-bond nature of the C-O-bond give suitable polarity and flexibility in the LC core [1,2]. Especially, the ester group has been known to make evolutions of Smectic A and C (Sm A and Sm C, respectively) phases easily, so that frequently it has been used as a linkage of smectic LC materials, such as ferroelectric ones [3].

The intrinsic potential of the ester group for the enhancement of smectic properties has been interpreted in terms of polar interactions involving dipole and charge arising from the carboxyl group, but the detailed mechanism has not been clarified and is still mysterious [4,5]. Typical examples are shown in Figure 1.

According to quoted data, the relative length of both terminal hydrocarbon chains with respect to the orientation of the ester group(s) appears to determine the smectic properties. On the other hand, a lot of LC compounds incorporating a lateral substituent have been developed as materials for display devices. Among them, LC materials incorporating a polar substituent, such as a nitro or a cyano group, are also of special interest, since they also exhibit complex phase transition behavior [6–9].

Considering the fact that the ester and nitro groups have dipole moments of ca. 1.9 and 4.2 D, respectively, and that the dipole-dipole interaction

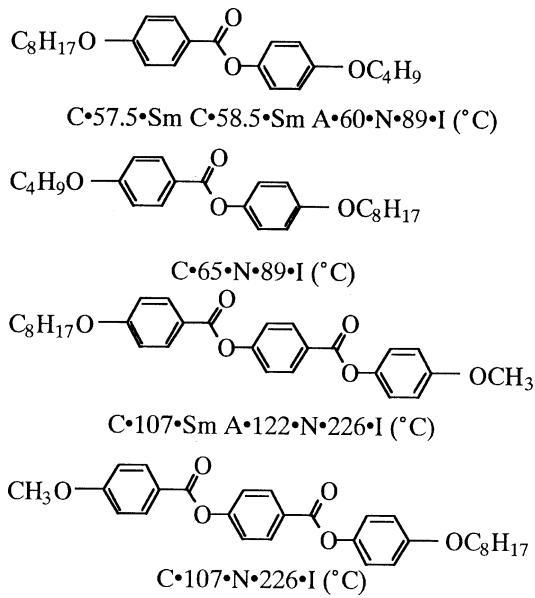

FIGURE 1 Phase transition behavior of ester compounds (T/°C). Data were cited from Demus and Zaschke [4] and Tasaka et al. [5].

is proportional to μ^2/R^3, where μ and R are dipole moment and the distance between dipoles, respectively, the dipole and/or charge of these groups must influence not only the thermal properties but also the molecular arrangement of smectic phases.

In our previous articles, we reported the mesomorphic properties of related compounds having a phenyl-X-phenyl-Y-phenyl core, where X, Y = COO, OOC [10–12]. In those articles, we described that in four isomeric compounds, the phenyl-X-phenyl-Y-phenyl core, the electrostatic nature of the terminal substituents, and the relative orientation of two ester groups notably affect not only the thermal properties but also the layer structure in the Sm phases. One noteworthy fact is that 4-alkoxyphenyl 4-(4-octyloxybenzoyloxy)benzoates easily exhibit both Sm A and Sm C phases even if the alkoxy chain is short and, on the contrary, it is hard for 4-octyloxyphenyl 4-(4-alkoxybenzoyloxy)benzoates to exhibit both phases. These compounds are different only in the orientation of two ester groups with respect to both terminal alkoxy groups. The other noteworthy fact is that 4-alkoxyphenyl 4-octyloxyphenyl terephthalates exhibit Sm A and Sm C phases from the lower homologs; conversely, it is hard for 4-(4-octyloxybenzoyloxy)phenyl 4-alkoxybenzoates to exhibit smectic phases. These compounds have a symmetric LC core.

In this article, we will call attention to the difference in the phase transition behavior for 1 and 2 in Figure 2 and further examine the layer structure of Sm A and Sm C phases by small-angle X-ray diffraction measurements.

In connection with the polar interaction, the phase transition behavior and the layer structure of 4-(4-octyloxybenzoyloxy)phenyl 3-nitro-4-alkoxybenzoates (3) and 4-(4-octyloxyphenoxycarbonyl)phenyl 4-alkoxy-3-nitrobenzoates (4) were also examined. We especially focused on the evolution and layer structure of the Sm C phase for **1**–**4**. The results

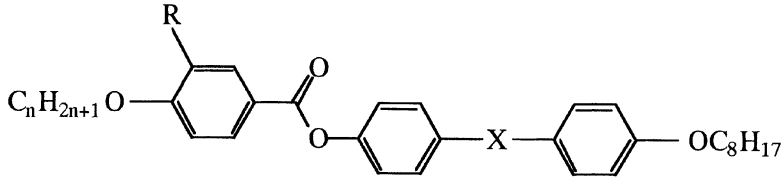

Compounds **1** R = H X = COO
2 R = H X = OOC
3 R = NO_2 X = COO
4 R = NO_2 X = OOC

FIGURE 2 Molecular structures of compounds **1**–**4**.

obtained by thermal, microscopic, and X-ray diffraction measurements are discussed in connection with the smectic properties and molecular parameters estimated by a semiempirical molecular orbital calculation.

EXPERIMENTAL

Materials

The homologous series of **1**–**4** were prepared by the conventional method described in our earlier article [11].

Methods

The transition temperatures and latent heats were determined using a differential scanning calorimeter, Seiko SSC-5200 DSC, where indium (99.9%) was used as a calibration standard (mp = 156.6°C, 28.4 J/g). The DSC thermogram was operated at a heating or a cooling rate of 5°C/min. The mesophases were characterized using a Nikon POH polarizing microscope fitted with a Mettler thermo-control system (FP-900), where temperature was calibrated by benzoic acid (mp = 122.4°C).

X-ray diffraction measurement for the smectic phases was performed using a Rigakudenki RINT 2200 diffractometer, where CuKα ($\lambda = 1.541$ Å) was used as an X-ray source. The reflection angle was calibrated by a comparison of both right and left angles. The temperature was controlled using a Rigaku PTC-20A thermo-controller. The samples which were put into in a quartz capillary (1.5 mmϕ) were oriented by a constant magnetic field (480 G). The samples were placed along the goniometer axis so that the counter movement in the recording plane allowed us to scan the nematic and smectic reciprocal lattice mode along q(q = 2π/d is the reciprocal space vector), i.e., in the direction parallel to the director **n**. The samples gradually decomposed above 200°C, so that the X-ray diffraction measurement was carried out below 190°C.

The molecular orbital parameters referred to in this article were obtained by a semiempirical molecular orbital calculation, MOPAC97, where minimization of the heat of formation was achieved by an AM1 method.

RESULTS AND DISCUSSION

Transition temperatures for **1**–**4** examined by microscopic observation and DSC thermogram are summarized in Table 1, and the transition temperatures are plotted against the carbon number in Figure 3, where most of the data were cited from Takenaka et al. [10] and Sugiura et al. [11].

TABLE 1 Transition Temperatures (°C) for **1**–**4**

	R	**n**	C		Sm C		Sm A		N		I
1	H	1	·	101	—		—		·	214	·
		4	·	99(	·	65)	—		·	207	·
		5	·	97	·	101	—		·	201	·
		6	·	96	·	132	·	144	·	198	·
		7	·	89	·	142	·	155	·	193	·
		8	·	84	·	142	·	163	·	188	·
2	H	1	·	124	—		—		·	224	·
		4	·	124	—		—		·	215	·
		5	·	115	—		—		·	205	·
		6	·	108	·	109	—		·	200	·
		7	·	112	·	119	—		·	197	·
		8	·	122	·	126	—		·	194	·
3	NO_2	1	·	141	—		—		·	166	·
		2	·	122	—		·	154	·	177	·
		3	·	96	—		·	160	·	173	·
		4	·	85	—		·	173	·	179	·
		5	·	87	(·	56)	·	179	—		·
		6	·	82	(·	69)	·	181	—		·
		7	·	75	·	113	·	180	—		·
		8	·	76	·	128	·	179	—		·
		9	·	71	·	142	·	176	—		·
4	NO_2	1	·	118	—		—		·	171	·
		2	·	116	—		—		·	178	·
		3	·	101	·	106	—		·	175	·
		4	·	76	·	114	—		·	172	·
		5	·	63	·	123	—		·	168	·
		6	·	87	·	139	—		·	169	·
		7	·	55	·	144	—		·	165	·
		8	·	64	·	150	—		·	164	·
		9	·	59	·	152	—		·	161	·

Parentheses indicate a monotropic transition. Data were cited from Takcnaka et al. [10] and Sugiura et al. [11].

In a previous paper [10], it has been reported that the smectic properties of the 4-R_1-phenyl 4-(4-R_2-benzoyloxy)benzoates (R_1 and R_2 = an alkoxy, or an alkyl group) are notably influenced by the chain length at R_2. When the alkoxy or the alkyl group at R_2 is suitably long—for example, an octyloxy group—it is easy for the homologs to exhibit the Sm A and Sm C phases even if the alkoxy and/or the alkyl group at R_1 is very short. When the hydrocarbon chain at R_2 is short (compounds **1**), on the contrary, it is difficult for the homologs to exhibit Sm phases, even if R_1 is the octyloxy group. Interestingly, the Sm C phase for **1** commences from the butoxy homolog, while the Sm A one commences from the hexyloxy one. This phase behavior may be a rare case.

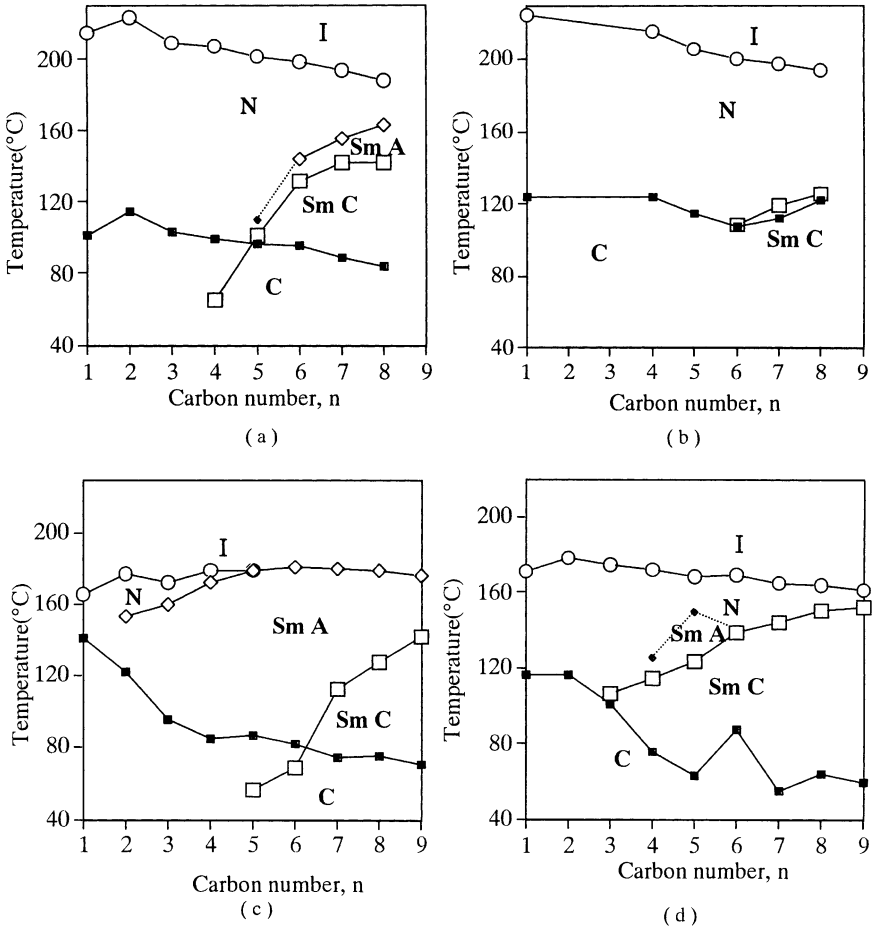

FIGURE 3 Plots of transition temperatures against carbon number, n, for (a) **1**, (b) **2**, (c) **3**, and (d) **4**, ○; N-I; ◇; Sm A-N(I); □, Sm C-Sm A(N) transitions. ◆ indicates a pseudo–Sm A-N transition point (see text). The dotted line indicates a pseudo Sm A-N transition.

We also reported that it is also difficult for 4-(4-R_1-phenoxy-carbonyl)phenyl 4-R_2-benzoates, **2**, to exhibit Sm phases. As shown in Figure 3(b), the Sm C phase commences from the hexyloxy homolog where, in addition, the Sm C-N transition temperature is low. These results indicate that the smectic properties are notably influenced by the relative orientation of two ester groups with respect to the terminal hydrocarbon chains.

As we can see from Figure 3(c), the phase transition behavior is also influenced by the nitro group at the lateral position, and the trend is especially notable in smectic properties. In compounds **3** the Sm A phase commences from the ethoxy homolog, and the Sm A-N (I) transition temperature stays almost constant through the homologs. On the other hand, the Sm C–Sm A transition temperature is rather reduced by the introduction.

In compounds **4** (Figure 3(d)), the introduction of the nitro group at the lateral position makes the evolution of the Sm C phase easy and results in a notable enhancement of the Sm C-N transition temperature. Although all the homologs did not exhibit the Sm A phase as far as microscopic and DSC measurements, X-ray examination suggested that in some homologs cybotactic domains have a layer structure of the Sm A phase exist near the Sm C-N transition points, as discussed in the later part of this article (see Figure 6). In this article, the N phase with the cybotacitc domains is termed a "pseudo-Sm A" one. The pseudo-Sm A phase was observed in the N phase of the butoxy-hexyloxy homologs of 4 and the pentyloxy homologs of **1**. The roughly estimated Sm A-N transition temperatures (pseudo-Sm A-N) are plotted by black diamonds in Figures 3(a) and 3(d).

It is well known that the texture of mesophases is influenced by physical conditions such as the molecular alignment on a glass surface, temperature, and the previous states. In this article we referred to the texture of the Sm C phase, since the Sm C phase is converted from different states in the cooling process.

The Sm A and Sm C phases of **1** commence from the butoxy and hexyloxy homologs, respectively. The texture of the Sm C phase for the butoxy and pentyloxy homologs of **1**, therefore, is derived from the schlierene texture of the N phase in the cooling process, and exhibits a fan one. The Sm C phase for the hexyloxy-octyloxy homologs of **1**, on the other hand, is derived from the Sm A phase and shows a metamorphic texture in the Sm A phase, i.e., a broken fan texture, in the cooling process. The Sm C phase for all homologs of **3** is derived from the Sm A phase in the cooling process, so that a metamorphic broken fan texture in the Sm A phase is formed in the Sm C phase. An example is shown in Figure 4(a).

All homologs of compounds **2** and **4** exhibit it only Sm C and/or N phases, so that the Sm C phase is derived from the schlierene texture of the N phase. The texture of the Sm C phase is shown in Figure 4(b), which is common in **2** and **4**. Apparently, a number of discontinuous lines exists within the fan texture. Of course, the Sm C phase shows the conventional schlierene texture under a homeotropic alignment.

A similar texture has been observed in a broken fan texture of smectic I, F, and G phases converted from the Sm C or Sm A phase [4]. That is, the texture appears to be common in the highly ordered tilt phases. Of course,

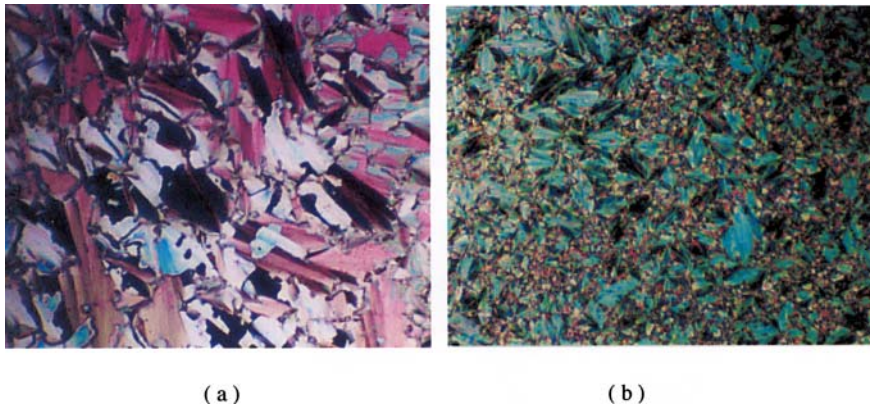

FIGURE 4 Micrographs for: (a) Sm C phase for the octyloxy homolog of **2** at 120°C; the texture was evolved from the schlierene one of the N phase in the cooling process, and (b) Sm C phase for the octyloxy homolog of **3** at 100°C; the texture was evolved from the fan texture of the Sm A phase. (See COLOR PLATE I)

the Sm C phase of the present compounds has no order within the smectic layer, as far as the X-ray results mentioned in the later part of this article. One of the possibilities is that the layer structure evolved from the N phase in the cooling process is so stable and unchangeable upon temperature change (see Figure 7) that the disagreement of the tilt layer within the fan can not be thermally dissolved. A similar texture is also exhibited by the Sm C phase for some derivatives of 3, where the Sm C phase is converted from an isotropic solution [15].

X-Ray Diffraction Studies

The layer structure of smectic phases was characterized by an X-ray diffraction method. The profiles of the Sm A and C phases for all of the compounds show two reflection peaks. One is observed as a sharp reflection peak near $2\theta = 2.5°$ arising from the layer plane, and the other is a broad one centered at ca. 20°. The latter peak was too broad and weak to calculate the maximum value. These results indicate that these two phases have no order of molecular arrangement within the smectic layer.

The temperature dependency of the layer structure for **1** has been reported in a previous paper [16]. The plots of the layer spacing versus temperature are shown in Figure 5(a).

The Sm C phase for compounds **2** commences from the hexyloxy homolog. The X-ray profiles for the hexyloxy, decyloxy, and octyloxy homologs show one reflection peak below the N-Sm C transition point, and

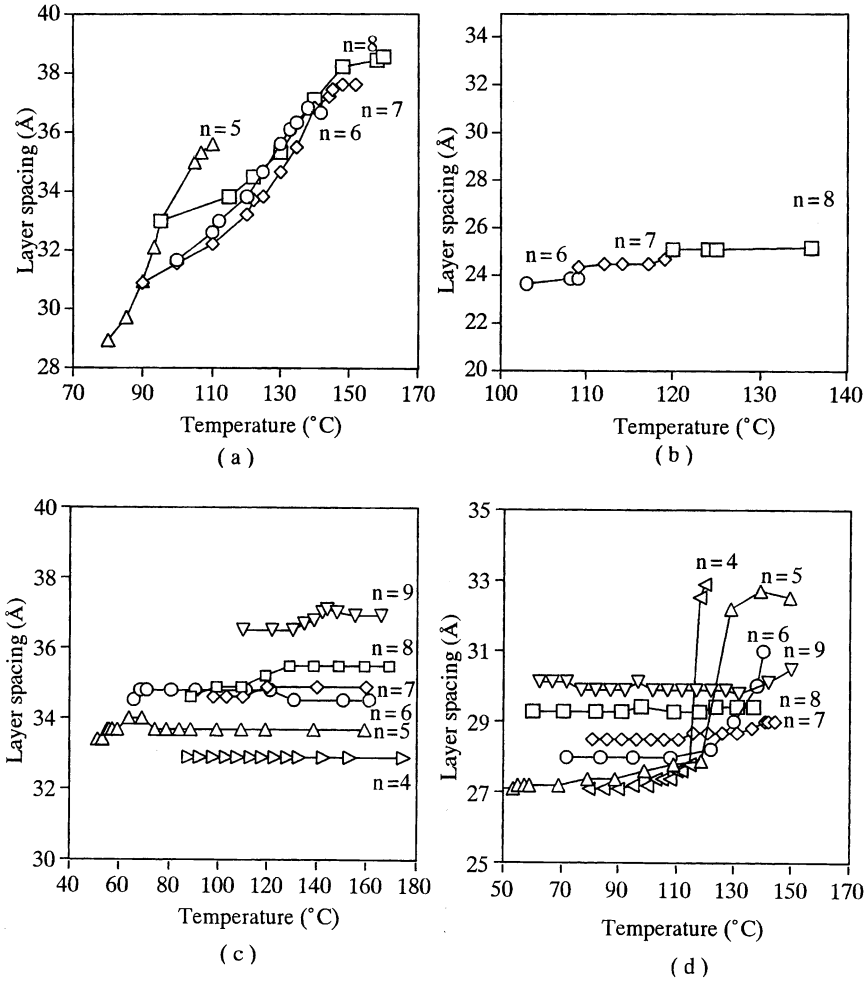

FIGURE 5 Plots of layer spacing versus temperature for (a) **1**, (b) **2**, (c) **3**, and (d) **4**. n indicates the carbon number of the alkoxy chain.

the peak intensity becomes slightly high with decreasing temperature. Interestingly, the layer spacing for **2** is almost independent of temperature through the Sm C range. The results are shown in Figure 5(b).

Compounds **3** have the mesomorphic sequence of Sm C–Sm A-N type. The profiles for the octyloxy homolog of **3** are shown in Figure 6.

The profile at 150°C shows a sharp reflection peak at $2\theta = 2.49°$ corresponding to 35.5 Å. The reflection angle stays almost constant through the Sm A (128°C) and Sm C (102°C) phases. At the low temperature region,

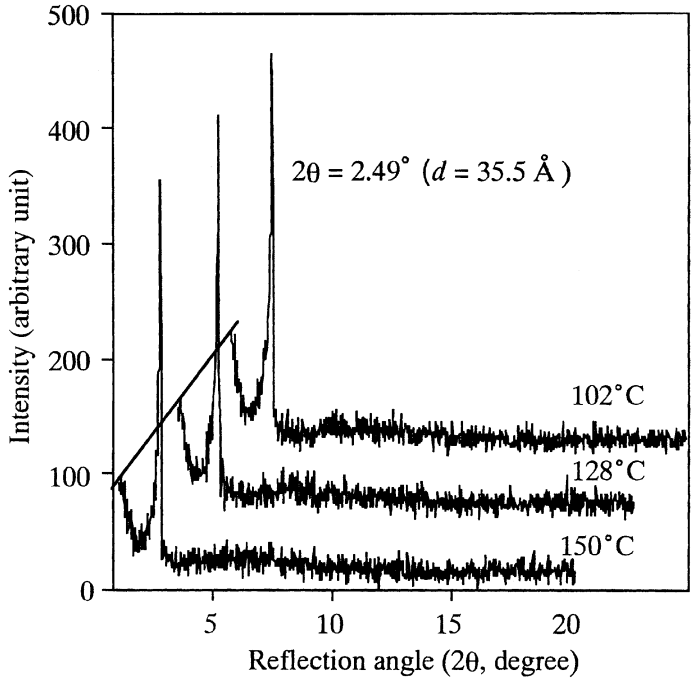

FIGURE 6 X-ray profiles of the octyloxy homolog of **3**.

the reflection peak is accompanied by a weak shoulder beside the small angle region, though it was not separated into any peak. Two facts are worthy of note for the homologs. One is that the plots for pentyloxy to nonyloxy homologs tend to exhibit an upward swelling near the Sm C-N transition point. Second is that the layer spacing stays almost constant through the Sm A and C phases, indicating that the layer structure is unchangeable through the Sm A and Sm C phases.

Some homologs of compounds **4** show an interesting phase transition behavior. The X-ray profiles for the pentyloxy homolog of **4** are shown in Figure 7 as examples.

As shown in Table 1, the pentyloxy homolog shows only Sm C and N phases. Interestingly, a broad reflection peak at 2.72° (32.5 Å) was observed even in the N phase (at 149 and 129°C), became intense and rapidly shifted to 3.22° (27.9 Å) at 122°C due to the evolution of the Sm C phase, and then became constant at 3.22° (27.4 Å). The broad reflection in the n phase should arise from the "pseudo Sm A" one mentioned above. A similar broad reflection peak in the N phase was observed in the butoxy and hexyloxy homologs. Another similar broad reflection peak is also observed in the

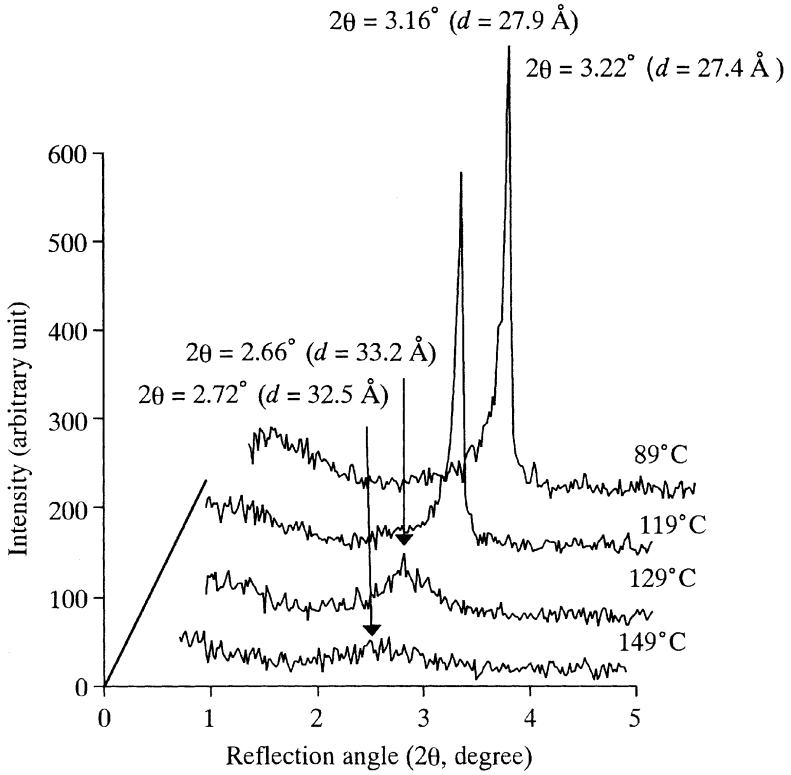

FIGURE 7 X-ray profiles of the pentyloxy homolog of **4**.

pentyloxy homolog of **1**, and the emerging points roughly estimated from the X-ray results are plotted as black diamonds in Figures 3(a) and 3(d). The layer spacing calculated from the peak top is plotted against temperature in Figure 5(d).

The layer spacing for the homologs of **1** in Figure 5(a) shows a notable temperature dependency, and becomes short with decreasing temperature. For the pentyloxy homolog of **1**, three points at the higher temperature region correspond to the layer spacing in the pseudo Sm A phase. The notable temperature dependency is common in conventional LC materials having the Sm C–Sm A phase transition, and explicable in terms of the continuous change of the tilt angle due to the Sm A–Sm C phase transition.

A noteworthy fact for **2** and **3** is that the layer spacing stays constant through the Sm A and Sm C phases. For compounds **4**, the notable change in the layer spacing for the butoxy, pentyloxy, and hexyloxy homologs arises from the evolution of the pseudo–Sm A phase.

Conformational Analysis and Molecular Arrangement

The conformation of **1** and **2** was estimated by a semiempirical molecular orbital calculation (MOPAC97), where the heat of formation was minimized by an AM1 method. In the conformational analysis the alkyl chains were supposed to have a zigzag conformation, since it gives the lowest heat of formation in the calculation. In practice, it would be reasonable to assume that the long hydrocarbon chain of LC molecules forms the zigzag conformation, giving a linear shape [12]. In addition, two ester linkages were supposed to form an s-trans conformation so as to keep the best linearity of the LC core. Under these assumptions, two extreme conformations for **1** and **2** are possible and illustrated in Figure 8.

The longest (down) and shortest (up) conformers of the octyloxy homologs of **1** and **2** are illustrated in Figures 8(a) and 8(b), respectively, where the energy difference between two conformers is almost zero, so that both conformers might be distributed in the LC phases. The longitudinal lengths for two extreme conformers calculated from the models are plotted versus in Figure 9.

For compounds **3** and **4**, the steric hindrance between the nitro group and the adjacent alkoxy group is so high (27.5 kJ/mol in the MO calculation) that the rotation of the alkoxy group must be strongly restricted. However, the entire molecular lengths for **3** and **4** are almost same as those for **1** and **2**, respectively. The molecular lengths for **3** and **4** are plotted in Figures 9(c) and 9(d).

Interestingly, as shown in Figure 9(a), the longitudinal length for the longest conformer is in very good agreement with the observed layer spacing for the Sm A phase, and the layer spacing for the Sm A phase of **1** varies along with the molecular length for the longest conformer, while the plot of the higher homologs deviates a little. These results indicate that among many possible conformers the longest (linear) conformer (down in Figure 8(a) and the related ones preferentially exist in the Sm A phase. This trend must be common in the other mesophases, such as those in N and Sm C.

On the other hand, the layer spacing for the Sm C phase exhibits a notable even-odd alternation, where the differences in the layer spacing between the pentlyoxy and hexyloxy, and heptylxoy and octyloxy homologs are 2.7 and 4.0 Å, respectively. Considering the C-C bond length of 1.51 Å for the hydrocarbon chain and that the entire molecular length increases 1.2 Å/CH_2 (1.51*cos(111/2), where 111° is the C-C-C bond angle for the hydrocarbon chain), the notable change in the layer spacing should be attributable to the change in the tilt angle in the Sm C phase. Supposing that the tilt angle, θ, in the Sm C phase is given by $\cos^{-1}$ ($d_{\mathrm{Sm\ A}}/d_{\mathrm{Sm\ C}}$) shown in Figure 10, a simple calculation gives tilt angles of 36.8°, 29.8°,

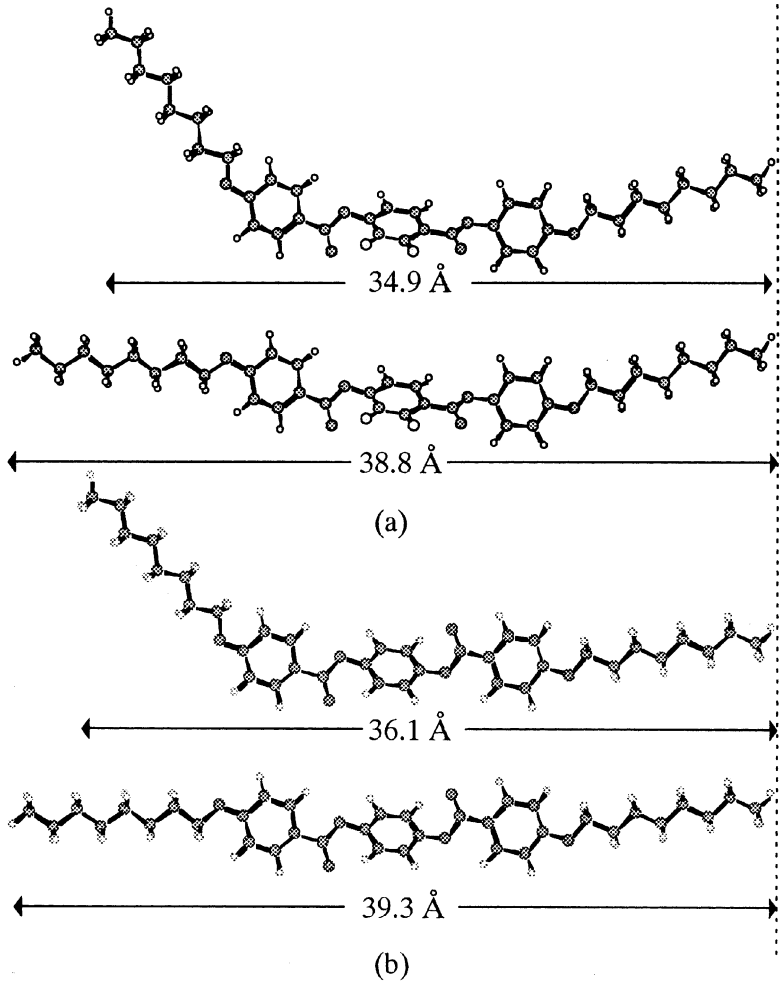

FIGURE 8 Two extreme conformers for the octyloxy homologs of (a) **1** and (b) **2**.

32.6°, and 21.7° for the pentyloxy, hexyloxy, heptyloxy, and octyloxy homologs, respectively. As shown in Figure 9(a), however, the plots of the layer spacing for the Sm A and Sm C phases gradually approach each other on ascending the homolog, indicating that the linearity of the alkoxy chains at both terminal positions gradually loses on ascending the homolog. The layer spacing for the Sm C phase of **2** is notably short compared with the calculated molecular length, and appears to increase linearly on ascending the homolog. Supposing that the layer spacing has a linear correlation with the carbon number, the plot gives a slope of 0.60 Å/CH_2.

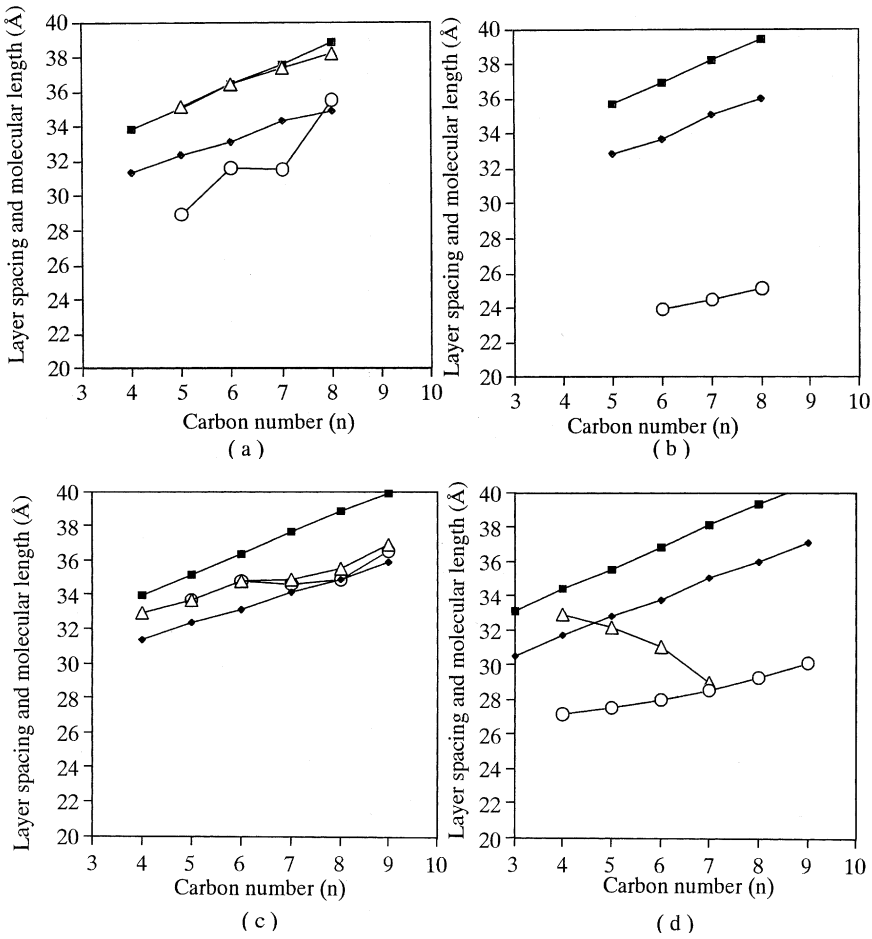

FIGURE 9 Plots of layer spacing and calculated molecular length versus carbon number for (a) **1**, (b) **2**, (c) **3**, and (d) **4**. ■ and ◆ indicate the longest and shortest molecular lengths calculated from the models in Figure 8, respectively. The layer spacing in the Sm C phase in Figure 9(a) was taken at Sm C–Sm A transition temperature −20°C. The layer spacing in the Sm A phase in Figures 9(a) and 9(d) was taken from the maximal values observed. △ and ○ indicate *d* for pseudo Sm A and Sm C phases, respectively.

The layer spacing of the Sm A phase for the earlier homologs of **3** has the intermediate value of the calculated molecular lengths between both longest and shortest conformers, and approaches that of the shortest conformer with a subtle curve after the hexyloxy homolog. Interestingly, the plot for the Sm C phase follows that for the Sm A phase, and the

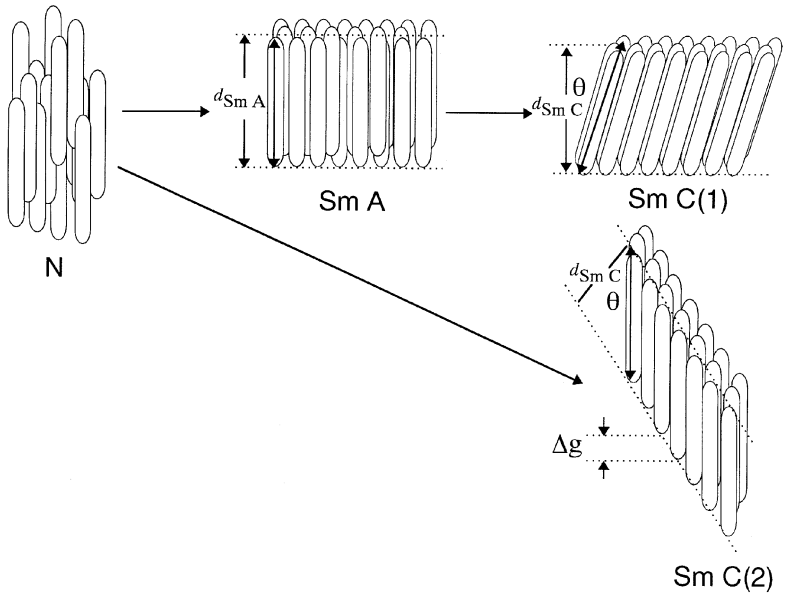

FIGURE 10 Molecular arrangement models in N, Sm A, and Sm C phases. $d_{Sm\ A}$ and $d_{Sm\ C}$ indicate the layer spacing in the Sm A and Sm C phases, respectively. θ indicates the tilt angle in the Sm C phase. The bar with arrows at both terminals represents the optical axis of the molecule. Δg indicates the gap in the molecular arrangement (see text).

characteristic even-odd alternation which appeared in **1** is not inherited. These results suggest that the layer structure of the Sm C phase is different from that of **1**, and those of both the Sm A and Sm C phases resemble each other.

The layer spacing in the pseudo–Sm A phase for **4** in Figure 9(d) becomes short on ascending the homolog and merges with that in the Sm C phase, and then the pseudo–Sm A phase disappears at the heptyloxy homolog. On the other hand, the layer spacing of the Sm C phase increases linearly on ascending the homolog. Supposing that the layer spacing is proportional to the carbon number, the plot gives a slope of 0.60 Å/CH_2. The good agreement of the slope with that for **2** suggests that the layer structure in the Sm C phase of **2** is inherited by **4** even in the introduction of the lateral nitro group.

With reference to the molecular structure in Figure 9, the molecular packing models for N, Sm A, and Sm C phases and the phase transition scheme are postulated and illustrated in Figure 10.

In the figure two kinds of mechanisms are postulated for the evolution of the Sm C phase. One is that the Sm C phase (Sm C(1)) is evolved from the

Sm A one, where the tilt angel, θ, becomes large with decreasing temperature, and the layer spacing ($d_{\mathrm{Sm\ C}}$) is given by the function of the tilt angle, θ ($d_{\mathrm{SmA}}{}^{*}\cos\theta$). Probably compounds **1** belong to this case, as shown in Figure 9(a). The other mechanism is that, on the other hand, the layer structure of the Sm C phase (Sm C(2)) is evolved directly from the N phase without passing through an orthogonal layer structure, such as the Sm A phase. The tilt layer structure (Sm C(2) in Figure 10) is evolved by the regular molecular rearrangement in the N phase and, therefore, the tilt angle may not exist in practice. So, the layer structure and the layer spacing evolved by this mechanism are almost independent of temperature, just like **2** and **4**. For the octyloxy homolog of **2**, the tilt angle in appearance is calculated to be 50.4° ($\cos^{-1}$ 25.1/39.4). Supposing that the molecular distance within the layer of the Sm C phase is ca. 4.6 Å', then the gap, Δg, between the adjacent molecules in the Sm C(2) model in Figure 10 is calculated to be 5.5 Å. The value of 5.5 Å corresponds to the diameter of one benzene ring and, interestingly, the postulated model (Sm C(2)) is similar to the crystalline structure of the octyloxy homolog of **4** [17,18].

The layer evolution and structure of the Sm C phase for **4** are assumed to be fundamentally similar to those for **2**, since Figures 9(b) and 9(d) show a similar feature to each other and their slopes are almost the same. The average tilt angle for six homologs is calculated to be 41° smaller by 10° than that for **2**. Considering the fact that **4** have a bulky nitro group at the lateral position, the molecular distance within the Sm C phase might be larger than that for **2**. Therefore, the Sm C phase is assumed to have a similar layer structure to the Sm C(2) model, where Δg is ca. 4 Å, supposing that the interdistance within the smectic layer is 4.6 Å. In the Sm C(1) and Sm C(2) models in Figure 10, LC molecules are illustrated by a rod, that is, a symmetric structure. In practice, present LC materials are dissymmetric except for **2**. To be specific, compounds **2** are dissymmetric except for the octyloxy homolog. Compounds **3** and **4** must be dissymmetric in regard to molecular shape and electrostatic nature due to the lateral nitro group. Nevertheless, the layer spacing for **2** and **4** linearly changes against the carbon number, as shown in Figures 9(b) and 9(d). These results indicate that the dissymmetry around two terminal alkoxy groups substituted at both terminal positions cannot be distinguishable in the Sm C phase. On the other hand, the alkoxy groups substituted at both terminal positions in phenyl benzoate and related systems having dissymmetry within the LC core have a different function [4,5] for the evolution and the thermal stability of the Sm A and Sm C phases, as shown in Figure 1. From these results, we assume that the symmetry of the LC core and the alkoxy chains at both terminal positions play some important roles for the layer formation and structure, such as the Sm A and Sm C phases, as well as the polar interactions around the ester groups.

The substitution of the lateral nitro group results in notable changes of thermal properties and layer structure (Figures 3 and 9). We feel that the electrostatic interactions near the nitro group affect the LC properties, and at the same time, the change in the entire molecular shape due to substitution is also an important factor. There is no doubt that the polar effect of the nitro group facilitates the evolution of the layer structure, but the detailed mechanism is now in consideration.

REFERENCES

[1] Kelker, H., & Hatz, R. (1980). *Handbook of Liquid Crystals*, Schumann, C. (Ed.). Verlag Chemie, 174.
[2] Gray, G. W., & Goodby, J. W. (1984). *Smectic Liquid Crystals*, Heyden and Son.
[3] Goodby, J. W. (1991). *Ferroelectric Liquid Crystals*, Goodby, J. W., Blinc, R., Clark, N. A., Lagerwall, S. T., Osipov, M. A., Pikin, S. A., Sakurai, T., & Yoshino, K., Zeks, B. (Eds.). Philadelphia: Gordon and Breach Science Publishers, 99.
[4] Demus, D., & Zaschke, H. (1976). *Flüssige Kristalle in Tabellen vol. 1*, Leipzig: VEB Deutscher Verlag für Grundstoff Industrie.
[5] Tasaka, T., Okamoto, H., Petrov, V. F., & Takenaka, S. (2001). *Liquid Crystals*, *28*, 1025.
[6] Gray, G. W., Jones, B., & Marson, F. (1957). *J. Chem. Soc.*, 393.
[7] Kutsumizu, S., Ishikawa, T., Nojima, S., & Yano, S. (1999). *Chem. Commun.*, 1181.
[8] Tasaka, T., Okamoto, H., Morita, Y., Kasatani, K., & Takenaka, S. (2002). *Chem. Lett.*, 222.
[9] Sugiura, H., Sakurai, Y., Masuda, Y., Takeda, H., Kusabayashi, S., & Takenaka, S. (1991). *Liquid Crystals*, *3*, 441.
[10] Takenaka, S., Sakurai, Y., Takeda, H., Ikemoto, T., Miyake, H., Kusabayashi, S., & Takagi, T. (1990). *Mol. Cryst. Liq. Cryst.*, *178*, 103.
[11] Sugiura, H., Sakurai, Y., Masuda, Y., Takeda, H., Kusabayashi, S., & Takenaka, S. (1991). *Liquid Crystals*, *9*, 441.
[12] Duan, M., Tasaka, T., Okamoto, H., & Takenaka, S. (2000). *Liquid Crystals*, *27*, 1195.
[13] Tasaka, T., Okamoto, H., Petrov, V. F., & Takenaka, S. (2001). *Mol. Cryst. Liq. Cryst.*, *357*, 67.
[14] Gray, G. W., & Goodby, J. W. (1984). *Smectic Liquid Crystals*, Philadelphia: Heyden & Son Inc., 1–124.
[15] Tasaka, T., Wu, J., Morita, Y., Okamoto, H., & Takenaka, S., unpublished results.
[16] Tasaka, T., Okamoto, H., Morita, Y., Kasatani. K., & Takenaka, S., *Liquid Crystals*, in press.
[17] Tamura, K., & Hori, K. (2000). *Bull. Chem. Soc. Jpn.*, *73*, 843.
[18] Tamura, K., Uchida, H., & Hori, K. (1999). *Mol. Cryst. Liq. Cryst.*, *330*, 1445.